Collisional Energy Transfer of NO D $^2\Sigma^+$ ($v' = 0$) and A $^2\Sigma^+$ ($v' = 4$) by O_2, N_2, Ar, and NO

Jorge Luque and David R. Crosley*

Molecular Physics Laboratory, SRI International, 333 Ravenswood Avenue, Menlo Park, California 94025

Received: September 7, 1999; In Final Form: January 20, 2000

Temporally and spectrally resolved fluorescence from NO D $^2\Sigma^+$ $v' = 0$ and A $^2\Sigma^+$ $v' = 4$ after two-photon excitation is studied in the presence of O_2, N_2, Ar, and NO colliders at room temperature. Quenching rate constants are determined for these gases. Nitrogen is found to efficiently quench these levels, with rate constants of $(2.6 \pm 0.2) \times 10^{-10}$ cm^3 s^{-1} and $(2 \pm 0.15) \times 10^{-11}$ cm^3 s^{-1}, respectively. The large quenching rate for A $^2\Sigma^+$ $v' = 4$ by N_2 compared to those of lower vibrational levels is explained by the onset of near resonant energy transfer into the N_2 A $^3\Sigma_u^+$ metastable state, similar to the path known for quenching the C $^2\Pi$ and D $^2\Sigma^+$ states.

1. Introduction

Nitric oxide is a product of fossil fuel combustion and of natural processes. Nitric oxides are important contributors to acid rain and are crucial to ozone formation and depletion mechanisms. Its presence in the atmosphere at trace levels, in some locations lower than 1 part per trillion, makes the detection and concentration quantification a nontrivial task.

Spectroscopic monitoring can be used to measure nitric oxide but requires a detailed knowledge of molecular band transition probabilities and collisional effects. The laser-induced fluorescence technique (LIF) depends on the dynamics in the excited state and requires an understanding of the collisional quenching processes. LIF is currently in use to detect NO quantitatively in the troposphere. Sandholm et al.[1] excite NO in a sequential two-photon process: in the first step, pumping from the ground state to the A state, and in a second, from the A to the D state, finally collecting the fluorescence from the D−X transition. This excitation is very selective, but it is rather complex because of the involvement of the dynamics of two different electronic states in the fluorescence quantum yield for this scheme. Although the technique is calibrated by seeding known amounts of NO in the inlet, a deeper knowledge of the underlying radiative and collisional processes is desirable.

The D $^2\Sigma^+$ state quenching is not known with certainty[2] except for rare gas colliders.[3] For example, the quenching rate constants by nitrogen and by nitric oxide quoted in the literature differ a factor of 5.[2,4,5] The main reason for the discrepancy is the relative experimental difficulty of time-resolved measurements in the nanosecond range; the radiative lifetime of NO D $v' = 0$ is ∼18 ns.[6,7] This problem forced most previous experiments to be carried out monitoring emission intensity instead, a method that is more prone to error. Conversely to the D $^2\Sigma^+$ state situation, A $^2\Sigma^+$ is more accessible and its electronic quenching by a wide range of colliders[8−10] and temperatures[11−13] is well-known for the low vibrational levels ($v' = 0-3$).[2,14] Sparse data are available for higher vibrational levels, where predissociation and energy transfer to other nearby electronic states (Figure 1) can change the behavior observed in the lower vibrational levels.

This paper summarizes time-resolved quenching measurements in the NO D $^2\Sigma^+$ $v' = 0$ and A $^2\Sigma^+$ $v' = 4$ with colliders, two of which are of interest in atmospheric measurements. We also examine the fate of the collisional deactivation by analysis of spectrally resolved fluorescence scans, finding different energy redistributions depending on the collider.

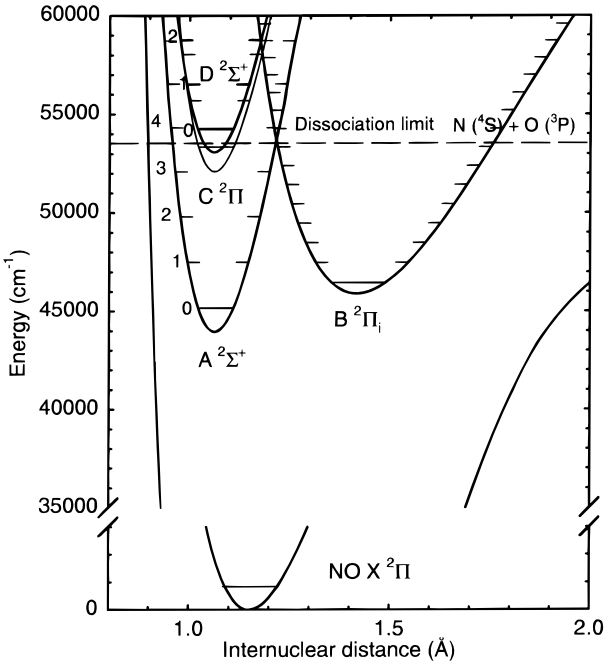

Figure 1. RKR potential energy curves for nitric oxide near the first dissociation limit.

2. Experiment

2.1. Experimental Details. The experiment is carried out in a flow cell with optical access. The gases are controlled by calibrated mass flowmeters (Hastings), and the total pressure in the cell is monitored with pressure transducers (MKS Instruments, Type 122A) having dynamic ranges up to 1000 Torr. The purity of the gases is 99.999% for argon and nitrogen, 99.995% for oxygen, and 99% for nitric oxide.

The NO was excited using two-photon absorption. Laser pulses are generated by a Lambda-Physik LPD-3000 dye laser

10.1021/jp993159a CCC: $19.00
Published on Web 03/01/2000

with Exalite-376, pumped by a Spectra-Physics Nd:YAG GCR-4, which gives pulses of ~6 ns temporal and 0.2 cm^{-1} spectral bandwidths. Energies up to 6 mJ/pulse were measured with a joulemeter (Scientech), although typical measurements were carried out with ~ 1 mJ/pulse. The beam is focused into the flow cell with a 25 cm focal length lens to a diameter of 200 μm. The cell is equipped with quartz windows to collect the fluorescence perpendicular to the laser beam propagation. These photons are spectrally filtered by a monochromator (Digikrom 240, f/7, 220 nm blaze angle grating) and detected by a photomultiplier. We use Hammatsu R166UH and RCA 1P28A photomultipliers, both with nominal 2 ns rise times. However, we tested the time response with scattered laser light, finding a response 6 ns fwhm wide with the 1P28, but 10.5 ns fwhm with the R166UH. Fitting the decay to a single exponential, we found 2 ns inherent response time for the 1P28 and 4 ns for the R166UH. The 1P28 is thus the choice for the most demanding lifetime measurements, despite a lower quantum yield in the 200 nm region compared to the R166UH. The signals are amplified and sent to either a boxcar integrator (Stanford, SRS-250) or a digital oscilloscope with a 1 ns time resolution (Tektronix, TDS 350, 200 MHz, 1 Gsample/s).

The fluorescence was collected from specific vibrational bands to avoid interference from other band emissions. Detection bandwidths were trapezoidal and 3−4 nm wide. Most measurements in the D $v' = 0$ state were done in the D−X (0,3) band at 209 nm; for A $v' = 4$, either the A−X (4,3) band at 209 nm or (4,13) at 306 nm were used, both showing the same results. Fluorescence decays were averaged over 1000 laser shots, and the transients fit to monoexponential decays between 90 and 5% of the intensity, then deconvoluted by the system time response.

Typical pressures for dispersed fluorescence spectra were 100 Torr collider plus 1 Torr of nitric oxide. Spectral resolution of 1.5−2 nm fwhm is enough to vibrationally resolve A−X, C−X, and D−X bands, all of which appear in our spectra. Two separate boxcar gates on the same input provide discrimination between prompt (20 ns gate) and long-lived (600−3000 ns gate) fluorescence. Dispersed fluorescence scans were corrected by the system spectral responsivity calibrated with a standard deuterium lamp (Optronics).

2.2. Influence of Photoionization. Single-wavelength, two-photon excitation was used to prepare each of the initial excited levels in our experiment. This is often accompanied by secondary processes, ionization, and multiphoton dissociation, induced by the large laser fluences utilized in the excitation step. The D $^2\Sigma^+$ $v' = 0$ state has a considerable photoionization cross section[15] and it is easy to ionize nitric oxide via this state:

$$\text{NO D } (v' = 0) + h\nu\ (\sim 375\text{ nm}) \rightarrow \text{NO}^+ + \text{e}- \quad \sigma_I = 6 \times 10^{-18}\ \text{cm}^2 \quad (1)$$

After photoionization, electron−ion dissociative recombination can happen fast enough to produce N and O atoms.[16]

$$\text{NO}^+ + \text{e}^- \rightarrow \text{N} + \text{O} \quad k = 3 \times 10^{-7}\ \text{cm}^3\ \text{s}^{-1} \quad (2)$$

A numerical kinetic model for the D $v' = 0$ two-photon excitation was implemented to assess these photoionization effects;[17,18] that is, the potential influence of the ions or atoms. The two-photon absorption cross section for D−X(0,0) is not known, and we use that for A−X(0,0) by Burris et al.,[19] resulting in an approximate two-photon cross section for the $P_{11} + O_{21}$ bandhead of 10^{-48} cm^4 s. A Gaussian laser pulse and a laser fluence of 3 J/cm^2 are used. The excitation of 1 Torr of NO (3.23×10^{16} cm^{-3}) is followed by fluorescence, predissociation, quenching, and photoionization. The model estimates the production of no more than $\sim 3 \times 10^{11}$ cm^{-3} ion density, during the 20 ns D state lifetime will produce 6×10^8 cm^{-3} of N or O atoms, neither the ion nor atom concentration is high enough to distort fluorescence decays and dispersed scans. The NO A $v' = 4$ photoionization cross section is 20 times smaller than that of NO D $v' = 0$,[6] but interference from photoionization or other processes is still possible using high enough laser fluences. To minimize problems related to secondary processes during laser excitation, we work with laser fluences less than 3 J/cm^2 ($\sim 5 \times 10^8$ W cm^{-2} or $\sim 10^{27}$ photon cm^{-2} s^{-1}) whenever possible and check lifetime and dispersed fluorescence scans at different laser powers. Even for these conditions, we cannot rule out completely the existence of interference because a reasonable fluorescence signal-to-noise ratio might be accomplished only accompanied by significant photoionization. One worrisome case is competitive photoionization of the C $v' = 0$ state which is populated by energy transfer after excitation of either A $v' = 4$ or D $v' = 0$ at high pressure. Such transfer occurs instantaneously with the laser excitation, and because C $v' = 0$ has a large photoionization cross section ($\sim 3 \times 10^{-17}$ cm^{-2}),[15] its removal can be appreciable, competing with quenching and predissociation. Estimates of this error using the differential equation model show that the C $v' = 0$ state population may be underestimated as much as 20−60%, depending on the total pressure, collider, laser fluence, and initially populated state. By similar reasoning, the D $v' = 0$ state populated after excitation of the A $v' = 4$ is underestimated by less than 20%, because its photoionization cross section is 5 times smaller than that of the C state predissociative levels.[15]

3. Method

Two-photon excitation pumping with visible or near-ultraviolet light is a method commonly used to study NO spectroscopy, for states whose single-photon excitation lies in the vacuum ultraviolet. Two-photon LIF spectra of NO D−X(0,0) and NO A−X(4,0) bands have been illustrated in previous papers investigating transition probability and lifetime studies.[6] These two bands present multiple accidental overlapping in the 375 nm region, but their structure is resolvable with our laser bandwidth. We have not attempted to study the rotational dependence of the quenching. The lines selected for excitation were the $P_{11} + O_{21}$ bandhead ($J' \approx 9.5$) in the D−X (0,0) band and the $P_{21} + Q_{11}$ bandhead ($J' = 2.5-4.5$) in the A−X(4,0) band, which do not contain perturbed levels and were previously used in the transition probabilities study.

Analysis of the fluorescence decay rate pressure dependence (Figures 2 and 4) is given by the equation

$$\frac{1}{\tau} = \frac{1}{\tau_o} + k_Q^{NO} P_{NO} + k_Q^{M} P_M \quad (3)$$

where τ_0 is the NO excited-state collision-free lifetime, k_Q are the quenching rate constants, and P the gas pressure.

Low-resolution dispersed fluorescence scans are useful to estimate collisional and radiative transfer into various electronic and vibrational levels. If the i state is populated by laser excitation and the j state is populated by energy transfer from i, the time integrated fluorescence from both states is related to collisional transfer:

$$X_{i\rightarrow j} = \frac{I_j}{I_i}\frac{F_i}{F_j}\frac{\Phi_i}{\Phi_j(1-\Phi_i)} \quad (4)$$

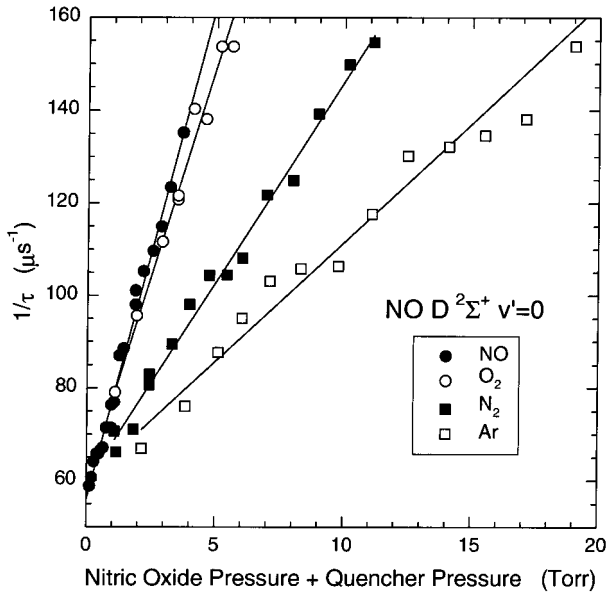

Figure 2. Inverse of the effective lifetime of NO D $v' = 0$ versus pressure of several colliders.

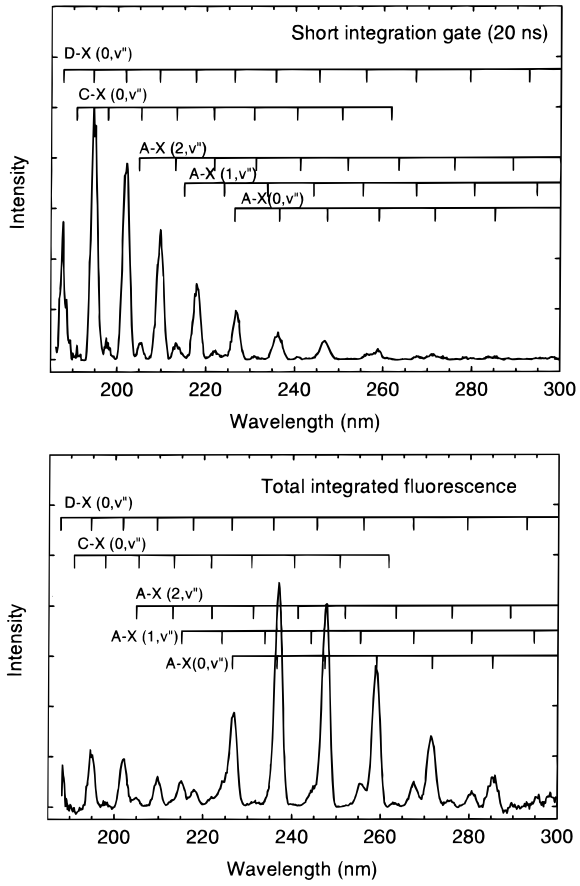

Figure 3. Dispersed fluorescence spectrum in the ultraviolet after pumping NO D $v' = 0$ in the presence of N_2. The resolution is 2 nm fwhm, and the pressure is 0.8 Torr of NO + 104 Torr of N_2. (upper panel) Integration time is 20 ns. Transfer D $v' = 0 \rightarrow$ C $v' = 0$ is detected. (lower panel) Late transfer to A $v' = 0$, 1, and 2 is observed with full time-integrated fluorescence (3 μs).

where $X_{i\rightarrow j}$ is the collisional transfer efficiency from the i state to the j state, I is the fluorescence intensity, F is the percentage collected of that state total fluorescence, and Φ the total fluorescence quantum yield. We examine the spectra looking for features of the A−X, B−X, C−X, and D−X systems.

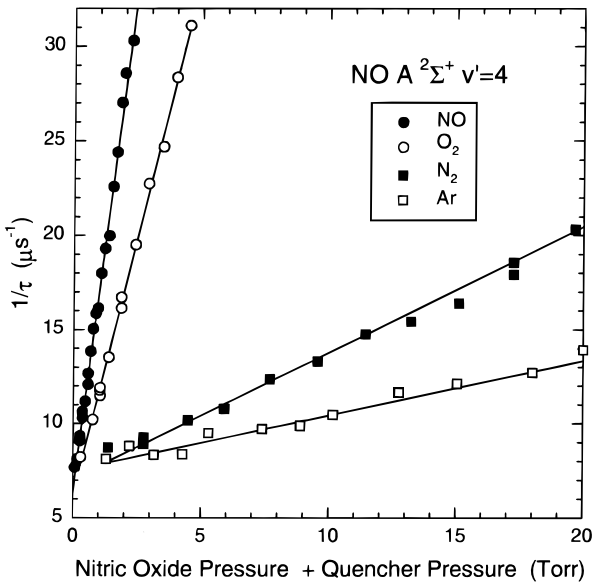

Figure 4. Inverse of the effective lifetime of NO A $v' = 4$ versus pressure of several colliders.

Einstein coefficients for the D−X and A−X transitions are from Luque and Crosley;[6] quenching rates for D and A states from Tables 1 and 2. C $v' = 0$ has a complex variation of fluorescence quantum yields with pressure because of the onset of predissociation for $J > {}^7/_2$ and the perturbation with B $^2\Pi_{3/2}$ $v' = 7$. Its radiative lifetime has been measured at 30 ns; Yagi[20] and Lahmani et al.[21] estimate a collision free fluorescence quantum yield of 0.1 for a room-temperature distribution in this predissociating state. Also, the C → A radiative cascade is taken into account to calculate the fraction of fluorescence measured.[21−24] The C $v' = 0$ quenching rates are taken from Asscher and Haas,[2] Imajo et al.,[5] and Callear and Smith.[25] NO, O_2, and N_2 removal rate constants are very similar to those for D $v' = 0$; the effective Ar quenching rate constant is $\sim 0.4 \times 10^{-11}$ cm^{-3} s^{-1}, nearly 4 times smaller than that of the D $v' = 0$ state.[25] Pressure dependence of the fluorescence quantum yield is highly dependent on the population distribution in the C state. This problem worsens for weak quenchers such as Ar, which induce predissociation through rotational transfer to dissociating levels.[21,25,26] Quantification of the B $v' = 0$ state quenching was not necessary because there was no noticeable signal from the B−X $(0,v")$ progression in the ultraviolet [although some A−X(2, $v"$) bands do overlap with the B−X $(0,v")$ bands below 300 nm, making the B $v' = 0$ state identification difficult].

4. Results and Discussion

4.1. NO D $v' = 0$ State. Table 1 displays the quenching rate constants measured here for the D $v' = 0$ state, with comparisons to other studies. The rate constant with nitric oxide is close to the values by Imajo et al., [5] Benoist et al.,[27] and Hikida et al.,[28] but much smaller than the values by Callear et al.[4] and Hikida et al.[29] Oxygen rates are in good agreement with the only other study done by Asscher and Haas.[2] Argon values agree well with the experiments by Chergui[3] and Callear et al.[4] However, nitrogen offers contradictory results. Ours is the only measurement using direct time decay of fluorescence. The study by Callear suggests a large quenching rate constant; but two later studies,[2,5] using two-photon excitation but also following the variation of the integrated intensity with pressure, give constants 5 times smaller than that early work. The present experiment,

TABLE 1: Quenching Rate Constants for NO D $v' = 0$; Units Are 10^{-10} cm^3 s^{-1}

collider	this work	Asscher and Haas[2 a]	Callear and Pilling[4]	Imajo et al.[5]	Chergui et al.[3]	Hikida et al.[28]	Benoist et al.[27]	Hikida et al.[29]
NO	6.6 ± 0.5	4.3 ± 0.8	35	7.2 ± 2.1		5.4 ± 1.5	8.0 ± 1.2	10.2 ±1.3
O_2	5.6 ± 0.5	6 ± 1						
N_2	2.6 ± 0.2	0.63 ± 0.13	2.8	0.5 ±0.1				
Ar	1.5 ± 0.2		1.5		1.3			

[a] Quenching rate constants in ref 2 were originally derived with a D $v' = 0$ lifetime of 25 ns using intensity Stern−Volmer plots. We correct them with the revised D $v' = 0$ state radiative lifetime value of 18.5 ns.

TABLE 2: Comparison of the Quenching Rate Constants for NO A $v' = 4$ and Lower A State Vibrational Levels; Units Are 10^{-10} cm^3 s^{-1}

collider	$v' = 0$	$v' = 1$	$v' = 2$	$v' = 3$	this work $v' = 4$	Hikida et al.[28] $v' = 4$
NO[14,40]	2.3 ± 0.2	2.6 ± 0.3	2.2 ± 0.3	2.3 ± 0.3	2.9 ± 0.4	2.7 ± 0.7
O_2[40]	1.6 ± 0.2	1.7 ± 0.2		1.6 ± 0.2	1.7 ± 0.2	
N_2[14]	0.0008	0.0043	0.008	0.023	0.2 ± 0.015	
Ar[14]	0.0004	∼0.0026	∼0.0026	∼0.0045	0.09 ± 0.01	
He[41]	0.0008	0.0008				0.0017 ± 0.0004

also with two-photon excitation but following the time-resolved fluorescence decays, obtains a value close to the work of Callear et al.

The quenching of D into the A state with N_2 is thought to happen by a nearly resonant energy transfer mechanism through the metastable state of N_2 A $^3\Sigma_u^+$:[30]

$$\mathrm{NO\ D}\ (^2\Sigma^+\ v' = 0) + \mathrm{N_2} \xrightarrow[k_1]{} \mathrm{N_2}\ (\mathrm{A}\ ^3\Sigma_u^+) + \mathrm{NO} \qquad (5)$$

$$\mathrm{NO} + \mathrm{N_2}\ (\mathrm{A}\ ^3\Sigma_u^+) \xrightarrow[k_2]{} \mathrm{NO}\ (\mathrm{A}\ ^2\Sigma^+) + \mathrm{N_2} \qquad (6)$$

$$\mathrm{NO}\ (\mathrm{A}\ ^2\Sigma^+) \xrightarrow[k_3]{} \mathrm{NO} + h\nu \qquad (7)$$

k_2 is slower than k_1 and k_3. We measured the time behavior of the NO A state and the dispersed fluorescence after excitation of NO D in 100 Torr of N_2. The time decay collected in the A−X(0,1) band has two components: a short one in the nanosecond range from the NO D−X(0,6) emission and the cascade to A $v' = 0$, and a long one in the microsecond range, due to transfer from N_2 (A) to NO (A). From the representation of the inverse of the long component lifetime versus the pressure of nitric oxide, we find a rate for N_2 (A) removal by NO, $k_2 = (5.5 \pm 1) \times 10^{-11}$ cm^{-3} s^{-1}, very close to a recent determination of $(6.9 \pm 0.7) \times 10^{-11}$ cm^{-3} s^{-1}.[31] The efficiency of the transfer from NO D $v' = 0$ to the A state by N_2 (A) is estimated from dispersed fluorescence scans (Figure 3) using the D−X(0,1), (0,2), and A−X(0,1) bands to be 65 ± 15%, slightly lower than the 82 ± 18% by Imajo et al.[5] and 96 ± 15% by Callear.[32] We find nearly 20% of the D state removal going to the NO C ($v' = 0$) state, which also transfers to N_2 with an efficiency of 42 ± 11%[5] via the same mechanism. Finally, the population ratio A ($v' = 0$)/A ($v' = 1$)/A ($v' = 2$) is 1.00:0.21:0.05 and is pressure independent after correcting for quenching and vibrational relaxation effects. This ratio is similar to results by Shibuya et al.,[31] once we adjust their values by the vibrational dependence of collisional removal of A v' levels by N_2 and NO as well. Piper et al.[33] measured the vibrational distribution produced in NO A after vibrationally selective relaxation of N_2 A $v' = 0$, 1, and 2. The maximum vibrational level available from D $v' = 0$ is N_2 A $v' = 2$. Using their state selective values, our NO A v' distribution suggests collisionally produced N_2-(A) with a large amount of population above $v' = 0$.

Oxygen and argon also produce electronic energy transfer to the C $v' = 0$ state, which accounts for at least 30% and 40% of the total collisional removal rate for those colliders, respectively. These observations for argon agree with the studies of Callear et al.,[4,14] Chergui and Le Duff,[3] and Lahmani et al.[21] Callear et al. estimate at nearly 100% the efficiency of the transfer D ($v' = 0$) → C ($v' = 0$) with argon. In our case, the value found is half as large, but the uncertainty in the C $v' = 0$ fluorescence quantum yield and potential competition with photoionization could account for the difference. Lahmani et al.[21] and Chergui and Le Duff[3] point out transfer from D $v' = 0$ to A $v' = 3$ with helium collider, but no such transfer was observed by us with argon, in agreement with Callear et al.[4] and Chergui and Le Duff.[3]

For tropospheric measurement purposes and assuming dry air, N_2 makes up 63% of the D $v' = 0$ state removal. Transfer to the metastable N_2 (A) happens efficiently, with ∼45% of the collisional removal going to N_2. The deactivation of N_2 (A) by O_2 is 5×10^{-12} cm^3 s^{-1},[34] 10 times slower than that of N_2. However, NO A $v' = 0$ is quenched strongly by oxygen, and the amount of fluorescence observable from N_2 A electronic transfer to NO A will be very small. Another issue is also related to the fluorescence detection bandwidth in tropospheric measurements, where NO D−X (0,0−1) emission is collected in the 184−197 nm range.[1,35] Our energy transfer studies show that nearly 4% of the light collected in that wavelength range comes from the C−X(0,0−1) bands, which are produced by C $v' = 0$ populated by electronic transfer from D $v' = 0$ by O_2 and N_2 colliders. The size of this contribution seems small enough that it can be disregarded as a potential problem for the current LIF detection scheme accuracy.

4.2. NO A $v' = 4$ State. As seen from Tables 1 and 2, all NO A $v' = 4$ state quenching rate constants are smaller than those of D $v' = 0$. There are no other experiments on A $v' = 4$ quenching with several colliders. Hikida et al.[29] measured the self-quenching of NO A $v' = 4$, finding the same result as in the present experiment. More interesting is the comparison with quenching from vibrational levels below $v' = 4$. There are two types of behavior depending on the quenching rate constant size. Good quenchers such as oxygen and nitric oxide have quenching constants fairly independent of vibrational level. On the other hand, the weak quenchers Ar and N_2 show for A $v' = 4$ at least a 10-fold increase compared to lower A state vibrational levels.

Dispersed fluorescence scans exciting A $v' = 4$ in the presence of NO or O_2 do not show appreciable transfer to D $v' = 0$, C $v' = 0$, and B $v' = 0$. This lack of electronic energy transfer is consistent with the lack of vibrational dependence

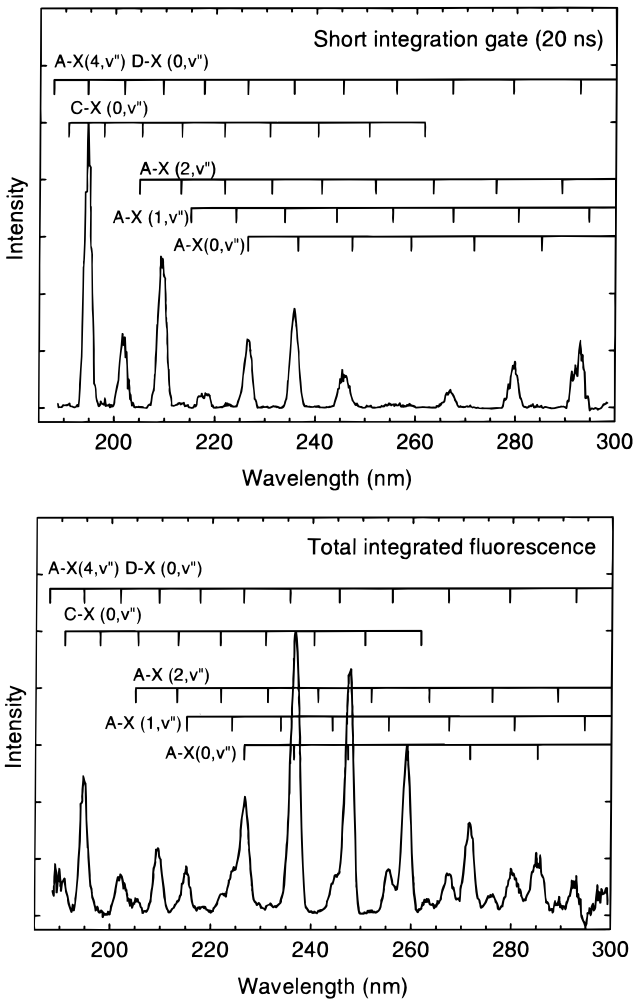

Figure 5. Dispersed fluorescence spectrum in the ultraviolet after pumping NO A $v' = 4$ in the presence of N_2. The resolution is 2 nm fwhm, and the pressure is 0.7 Torr of NO + 100 Torr of N_2. (upper panel) Integration time is 20 ns. The identification of the D−X(0,4) band indicates some A $v' = 4 \rightarrow$ D $v' = 0$ transfer. (lower panel) Late transfer to A $v' = 0$, 1, and 2 is observed with full time-integrated fluorescence (3 μs gate).

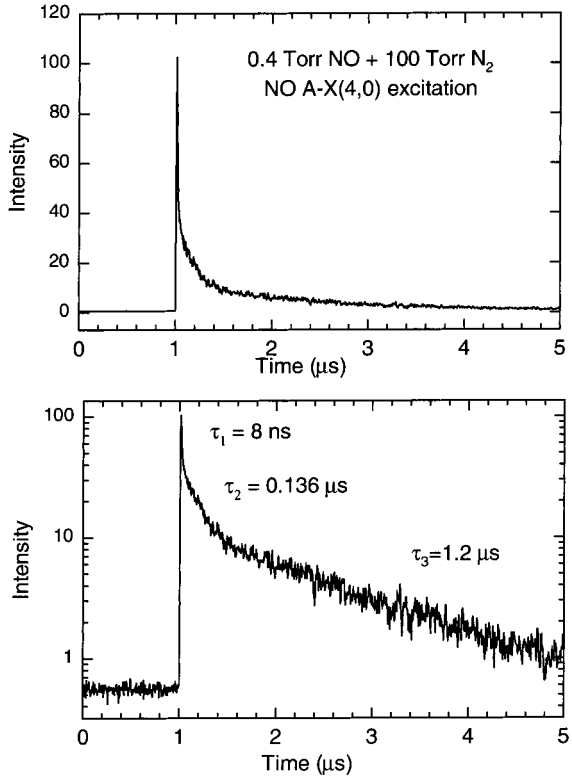

Figure 6. (upper panel) Temporal decay recorded in the NO A−X(0,1) (4,6), and (3,5) bands at 236 nm after excitation of the NO A $v' = 4$ band in a gas mixture of 0.4 Torr of NO and 100 Torr of nitrogen. (lower panel) Semilogarithmic representation of the same decay showing multiexponential behavior. The fast decay is emission from the optically populated A $v' = 4$, the intermediate component is likely due to direct electronic and vibrational transfer to other NO states, and the long component is A $v' = 0$ emission after transfer from the N_2 (A) metastable state.

of the quenching, since no new collisional paths are opened. Argon produces different spectra, where it is possible to identify C $v' = 0$, D $v' = 0$, A $v' = 0,1$ (A $v' = 0$ largely due to cascade from C $v' = 0$ and D $v' = 0$) and perhaps B $v' = 0$. It is not simple to reliably determine the quenching percentage going to these electronic states, due to the aforementioned complexities of Ar interacting with the C $v' = 0$ and possible D and C partial removal via photoionization. We estimate this transfer to be 50% of the total collisional removal, so it is reasonable to justify the larger A $v' = 4$ quenching rate compared to lower vibrational levels to be at least partially due to electronic transfer to nearby nitric oxide electronic states.

Nitrogen is the most interesting case. The behavior of A $v' = 0$ with this collider has been studied thoroughly and is a successful example of the charge-transfer model for collisional quenching proposed for the NO A state.[36] The change in quenching rate constant for the A $v' = 4$ state by 1 order of magnitude points out the onset of another more efficient quenching mechanism. Analyzing the dispersed fluorescence scans (Figure 5) we found that ~55% of the transfer goes to the A state lower vibrational levels. The time-decays recorded in the A−X(0,1) band show the same multiexponential behavior observed for the D state (Figure 6). These observations strongly suggest again the resonant energy transfer mechanism with the N_2 (A) metastable state as the likely mechanism. Also, the percentage of energy transfer to the D $v' = 0$ and C $v' = 0$ states is found to be ~10% and ~8%, respectively; thus, most of the transfer happens directly from A $v' = 4$ to N_2. The NO A $v' = 3$ level is above the N_2 A $v' = 0$ level, and it should be possible to observe the same resonant transfer. However, Imajo et al.[5] did not find the characteristic slower time behavior of the transfer N_2(A) + NO → NO (A) + N_2 after pumping A $v' = 3$. This apparently contradictory result may imply the existence of a low energy barrier for the energy transfer into N_2(A). It is important to recall that the A $v' = 4$ quenching rate constant is only 10% of the value for the isoenergetic D $v' = 0$, so factors other than just energy considerations play an important role in the total quenching rate.

The quenching rates are monitored with the A−X (4,3) or (4,13) bands, which have little overlap with bands from lower A v' levels. In these cases, the measured decay rate includes vibrational energy transfer as well. We use the dispersed fluorescence scans to evaluate the contribution of vibrational transfer for NO, Ar, and O_2 colliders, to be ~10%, 6%, and <1%, respectively. In the N_2 case, it is not possible to establish a certain value, but it is likely that there is a contribution from vibrational transfer because the population ratio A ($v' = 0$)/A ($v' = 1$)/A ($v' = 2$)/A ($v' = 3$) is 1:0.27:0.11:<0.07 is different from the one obtained from D $v' = 0$, 1.00:0.21:0.05 (compare Figures 3 and 5).

4.3. Atomic Recombination Chemiluminescence Effects. In some dispersed fluorescence scans, especially exciting the

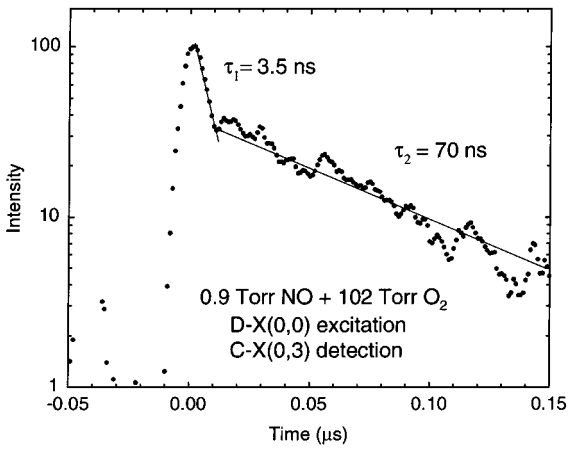

Figure 7. Semilogarithmic representation of the temporal decay recorded in the NO C−X(0,3) band at 213 nm (1.5 nm fwhm) after two-photon excitation of NO D $v' = 0$ using 2 mJ at 375 nm and focusing to 200 μm in a gas mixture of 0.9 Torr of NO and 102 Torr of oxygen. The fast decay is emission from C $v' = 0$ after transfer from D $v' = 0$. The slow decay is chemiluminescence from atomic recombination; the lifetime value of 70 ns is limited by NO and O_2 removal of N and O atoms.

D $v' = 0$ state with O_2 collider and less prominently with Ar, we observed long-lived emission from the C−X and A−X bands that cannot be accounted for by direct collisional transfer. We explain this observation by chemiluminescent emission. N and O atoms are known to recombine slowly producing chemiluminescence from the NO A, C, and B states:[16,37]

$$\mathrm{O + N + M \rightarrow NO\ (A,B,C,a,b,X,....) + M} \qquad k \approx 10^{-30}\ \mathrm{cm^6\ s^{-2}} \quad (8)$$

For example, when we excite the D state in the presence of collider M = O_2 at high pressures (>50 Torr), we observe unexpected long-lived emission of ~100 ns in the NO A−X and C−X bands; see Figure 7. Varying the pressure of nitric oxide and keeping the oxygen pressure constant, we obtain a rate constant of $\sim 7 \times 10^{-11}$ cm^3 s^{-1}, quite close to the value for the reaction[38,39]

$$\mathrm{N + NO \rightarrow N_2 + O} \quad k \approx 5 \times 10^{-11}\ \mathrm{cm^3\ s^{-1}} \qquad (9)$$

which acts like a limiting step for the N + O atomic recombination.

The most likely source of the N and O atoms in our system, leading to this chemiluminescence, is predissociation of the C $v' = 0$ state. This is known to be fast and in equilibrium with inverse predissociation.[25] This source can be active only when there is noticeable transfer to the C state. Such transfer occurs for D $v' = 0$ colliding with O_2 and Ar but does not happen in collisions of O_2 with A $v' = 4$. This explanation seems consistent with the A $v' = 4$ state dispersed fluorescence spectra with oxygen because chemiluminescence is not detected.

There are other processes leading to atomic production. One can be chemistry following photoionization. Another can occur in the O_2 plus NO system at high pressure and slow flow:[16]

$$\mathrm{2NO + O_2 \rightarrow 2NO_2} \quad k = 2 \times 10^{-38}\ \mathrm{cm^6\ s^{-1}} \qquad (10)$$

$$\mathrm{NO_2} + h\nu(375\ \mathrm{nm}) \rightarrow \mathrm{NO + O} \qquad (11)$$

This could provide an extra concentration of oxygen atoms and explain the enhancement of the chemiluminescence when exciting D $v' = 0$ at high pressure of oxygen collider. However, we have no direct evidence as to which mechanism, if any, dominates.

Acknowledgment. This work was sponsored by the NASA Global Tropospheric Experiment and the Atmospheric Chemistry Division of the National Science Foundation.

References and Notes

(1) Sandholm, S. T.; Bradshaw, J. D.; Dorris, Rodgers, K. S.; Davis, D. D. *J. Geophys. Res.* **1990**, *95*, 10155.
(2) Asscher, M.; Haas, Y. *J. Chem. Phys* **1982**, *76*, 2115.
(3) Chergui, M.; Duff, M. *Chem. Phys.* **1986**, *105*, 281.
(4) Callear, A. B.; Pilling, M. J.; Smith, I. W. M. *Trans. Far. Soc.* **1968**, *64*, 2296.
(5) Imajo, T.; Shibuya, K.; Obi, K.; Tanaka, I. *J. Phys. Chem.* **1986**, *90*, 6006.
(6) Luque, J.; Crosley, D. R. *J. Chem. Phys.* **1999**, *111*, 7405.
(7) Luque, J.; Crosley, D. R. *J. Chem. Phys.*, to be published.
(8) Greenblat, G. D.; Ravishankara, A. R. *Chem. Phys. Lett.* **1987**, *136*, 501.
(9) Paul, P. H.; Gray, J. A.; Durant, J. L., Jr.; Thoman, J. W., Jr. *Chem. Phys. Lett.* **1996**, *259*, 508.
(10) Furlanetto, M. R.; Thoman, J. W.; Gray, J. A.; Paul, P. H.; Durant, J. L. *J. Chem. Phys.* **1994**, *101*, 10452.
(11) Drake, M. C.; Ratcliffe, J. W. *J. Chem. Phys.* **1993**, *98*, 3850.
(12) Zhang, R.; Crosley, D. R. *J. Chem. Phys.* **1995**, *102*, 7418.
(13) Raiche, G. A.; Crosley, D. R. *J. Chem. Phys.* **1990**, *92*, 5211.
(14) Callear, A. B.; Pilling, M. J. *Trans. Faraday Soc.* **1970**, *66*, 1618.
(15) Rottke, H.; Zacharias, H. *J. Chem. Phys.* **1985**, *83*, 4831.
(16) Eichwald, O.; Yosufi, M.; Hennad, A.; Benabdessadok, M. D. *J. Appl. Phys.* **1997**, *82*, 4781.
(17) Mallard, W. G.; Miller, J. H.; Smith, K. C. *J. Chem. Phys.* **1982**, *76*, 3483.
(18) Brockhaus, A.; Yuan, Y.; Behle, S.; Engermann, J. *J. Vac. Sci. Technol. A* **1996**, *14*, 1882.
(19) Burris, J.; McGee, T. J.; McIlrath, T. J. *Chem. Phys. Lett.* **1983**, *101*, 588.
(20) Yagi, S.; Hikida, T.; Mori, Y. *Chem. Phys. Lett.* **1978**, *56*, 113.
(21) Lahmani, F.; Lardeux, C.; Solgadi, D. *Chem. Phys. Lett.* **1981**, *81*, 531.
(22) Scheingraber, H.; Vidal, C. R. *J. Opt. Soc. Am. B* **1985**, *2*, 343.
(23) Asscher, M.; Haas, Y.; *Chem. Phys. Lett.* **1978**, *59*, 231.
(24) Groth, W.; Kley, D.; Schurath, U. *J. Quant. Spectrosc. Radiat. Transfer* **1971**, *11*, 1475.
(25) Callear, A. B.; Smith, I. W. M. *Discuss. Faraday Soc.* **1964**, *37*, 96.
(26) Le-Duff, Y.; Chergui, M.; Boursey, E.; Schwentner, N. *Chem. Phys. Lett.* **1986**, *127*, 557.
(27) Benoist, O.; Lopez-Delgado, R.; Tramer, A. *Chem. Phys.* **1975**, *9*, 327.
(28) Hikida, T.; Suzuki, T.; Mori, Y. *Chem. Phys.* **1987**, *118*, 437.
(29) Hikida, T.; Yagi, S.; Mori, Y. *Chem. Phys.* **1980**, *52*, 399.
(30) Callear, A. B.; Smith, I. W. *Trans. Faraday. Soc* **1965**, *61*, 2383.
(31) Shibuya, K.; Imajo, T.; Obi, K.; Tanaka, I. *J. Phys. Chem.* **1984**, *88*, 1457.
(32) Callear, A. B.; Wood, P. M. *Trans. Faraday Soc.* **1971**, *67*, 272.
(33) Piper, L. G.; Cowles, L. M.; Rawlings, W. T. *J. Chem. Phys.* **1986**, *85*, 3369.
(34) Clark, W. G.; Setser, D. W. *J. Phys. Chem.*, **1980**, *84*, 2225.
(35) Sandholm, S.; Smyth, S.; Bai, R.; Bradshaw, J. *J. Geophys. Lett.* **1997**, *102*, 28651.
(36) Thoman, J. W.; Gray, J. A.; Durant, J. L.; Paul, P. H. *J. Chem. Phys.* **1992**, *97*, 8156.
(37) Matveev, A. A.; Parvilov, A. M.; Vilesov, A. F. *Chem. Phys. Lett.* **1994**, *217*, 582.
(38) Umemoto, H.; Hachiya, N.; Matsunaga, E.; Suda, A.; Kawasaki, M. *Chem. Phys. Lett.* **1998**, *296*, 203.
(39) Lee, J. H.; Michael, J. V.; Payne, W. A.; Stief, L. J. *J. Chem. Phys.* **1978**, *69*, 3069.
(40) Melton, L. A.; Kemplerer, W. *Planet. Space Sci.* **1972**, *20*, 157.
(41) Broida, H. P.; Carrington, T. *J. Chem. Phys.* **1963**, *38*, 136.